Induction of Androgen Formation in the Male by a TAT-VDAC1 Fusion Peptide Blocking 14-3-3ε Protein Adaptor and Mitochondrial VDAC1 Interactions

Yasaman Aghazadeh[1,2], Daniel B Martinez-Arguelles[1,2], Jinjiang Fan[1,2], Martine Culty[1-3] and Vassilios Papadopoulos[1–5]

[1]The Research Institute of the McGill University Health Centre, Montreal, Quebec, Canada; [2]Department of Medicine, McGill University, Montreal, Quebec, Canada; [3]Department of Pharmacology and Therapeutics, McGill University, Montreal, Quebec, Canada; [4]Department of Biochemistry, McGill University, Montreal, Quebec, Canada; [5]Department of Pathology, McGill University, Montreal, Quebec, Canada

Low testosterone (T), a major cause of male hypogonadism and infertility, is linked to mood changes, fatigue, osteoporosis, reduced bone-mass index, and aging. The treatment of choice, T replacement therapy, has been linked with increased risk for prostate cancer and luteinizing hormone (LH) suppression, and shown to lead to infertility, cardiovascular diseases, and obesity. Alternate methods to induce T with lower side effects are desirable. In search of the mechanisms regulating T synthesis in the testes, we identified the 14-3-3ε protein adaptor as a negative regulator of steroidogenesis. Steroidogenesis begins in mitochondria. 14-3-3ε interacts with the outer mitochondrial membrane voltage-dependent anion channel (VDAC1) protein, forming a scaffold that limits the availability of cholesterol for steroidogenesis. We report the development of a tool able to induce endogenous T formation. Peptides able to penetrate testes conjugated to 14-3-3ε site of interaction with VDAC1 blocked 14-3-3ε-VDAC1 interactions while at the same time increased VDAC1-translocator protein (18 kDa) interactions that induced steroid formation in rat testes, leading to increased serum T levels. These peptides rescued intratesticular and serum T formation in adult male rats treated with gonadotropin-releasing hormone antagonist, which dampened LH and T production.

Received 31 January 2014; accepted 16 June 2014; advance online publication 22 July 2014. doi:10.1038/mt.2014.116

INTRODUCTION

Reduced serum testosterone (T) is common among subfertile and infertile young men, including most men diagnosed with idiopathic infertility. Reduced T is also common in aging men, with T levels declining at age 40 and been low in the majority of men older than 60.[1,2] Reduced T is often associated with mood changes, fatigue, depression, decreased lean body mass, reduced bone mineral density, increased visceral fat, metabolic syndrome, decreased libido, and reduced sexual function.[1,3] T replacement therapy (TRT) is used clinically to restore T levels. TRT can treat symptoms associated with low T.[2,4,5] However, TRT may increase the risk and aggressiveness of prostate cancer,[2,6,7] augment the incidence of adverse cardiovascular events, favor obesity and depression and even increase the rate of mortality in patients.[3,4,8,9] Therefore is not recommended for patients at high risk of such diseases. Moreover, long-term TRT can suppress luteinizing hormone (LH) production, making this approach inappropriate for men who wish to have children. Fluctuating T levels, skin irritation, and T transfer to others through skin contact are additional disadvantages of TRT.[10] The molecular mechanisms that govern androgen formation in testicular Leydig cells remain unclear. Identification of these mechanisms will facilitate the development of new approaches for inducing endogenous T synthesis voiding exogenous T treatment.

T production is regulated by LH and its secondary messenger, cyclic adenosine monophosphate (cAMP). Cholesterol import from cytosolic sources into mitochondria is a hormone-sensitive and rate-limiting step of steroidogenesis. Cholesterol is cleaved into pregnenolone by CYP11A1 in mitochondria, and steroidogenesis begins. Cholesterol import into mitochondria is mediated by a hormone-induced multiprotein complex called the transduceosome, which is composed of cytosolic and outer mitochondrial membrane (OMM) proteins that control the rate of cholesterol entry into the OMM.[11] These proteins include the cytosolic mitochondria-targeted, hormone-induced steroidogenic acute regulatory protein (STAR),[12] the OMM high-affinity cholesterol-binding protein translocator protein (TSPO),[13] which contains a cholesterol recognition/interaction amino acid consensus (CRAC),[14] and the OMM voltage-dependent anion channel protein (VDAC1).[14,15] Recent studies shed light on the importance of interactions between STAR, TSPO, and VDAC1, suggesting that cholesterol import into mitochondria relies on the function and physical interactions between components of the transduceosome.[16–18] The nature and dynamics of transduceosome protein–protein interactions remain unknown.

Correspondence: Vassilios Papadopoulos, The Research Institute of the McGill University Health Center, Montreal General Hospital, 1650 Cedar Avenue, C10–148, Montreal, Quebec H3G 1A4, Canada. E-mail: vassilios.papadopoulos@mcgill.ca

The 14-3-3 family of adaptor proteins were recently shown to have binding motifs on important functional sites on STAR, TSPO, and VDAC1 and 14-3-3γ was identified as a regulator of STAR activity.[19] However, this hormone-induced 14-3-3 isoform was shown to function in a transient manner at the initiation of steroidogenesis, to delay the maximum STAR activity. Indeed, the function of 14-3-3γ is terminated as it dissociates from STAR, allowing for maximal steroid production. In these studies, the levels of the 14-3-3 family ε isoform, were found to be increased in Leydig cell mitochondria during steroidogenesis.[19] This isoform mediates in a tissue/target-specific manner, cell functions such as neural development,[20] adipocyte differentiation,[21] protein trafficking, cell cycle, apoptosis,[22] and cell signaling.[23] Levels of 14-3-3ε, formerly known as mitochondrial import stimulating factor,[24] are also high in human testes (http://biogps.org), but its function in this tissue is unknown. Herein, we report that 14-3-3ε serves as a scaffold protein regulating interactions between the transduceosome proteins, resulting in T formation. Pharmacological manipulation of these interactions leads to *in vivo* LH-independent T formation.

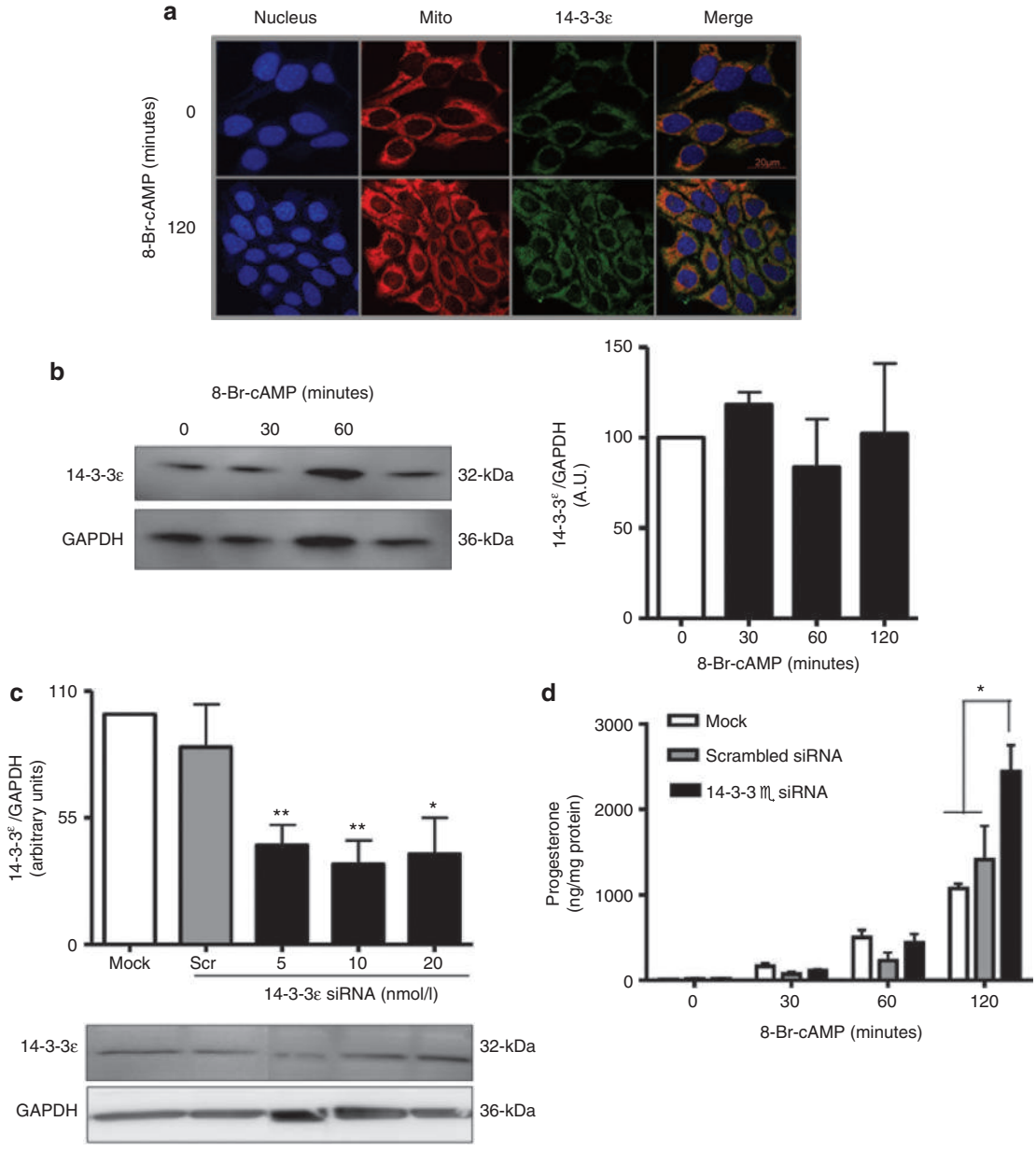

Figure 1 14-3-3ε is a negative regulator of steroidogenesis. (**a**) Immunocytochemistry indicates that 14-3-3ε is present in MA-10 cells (green) and that this protein partially localizes with mitochondria (red). MA-10 nucleus is shown in blue. (**b**) Immunoblot results of MA-10 cells stimulated with 8-Br-cAMP for indicated time points show 14-3-3ε expression and quantification relative to GAPDH control protein. (**c**) Immunoblot analysis indicating the levels of 14-3-3ε protein compared to glyceraldehyde 3-phosphate dehydrogenase (GAPDH) in MA-10 cells in the absence of siRNA (mock), transfected with scrambled or HPRT siRNA as negative and positive control, respectively, or transfected with a mixture of 14-3-3ε specific siRNA at different concentrations (20, 10, or 5 nmol/l). (**d**) MA-10 cells were transfected with 10 nmol/l 14-3-3ε siRNA and further stimulated with 8-Br-cAMP for 0, 30, 60, and 120 minutes, and progesterone levels were measured at each time point. *$P < 0.05$; **$P < 0.01$; ***$P < 0.001$.

RESULTS

14-3-3ε negatively regulates steroidogenesis

The hormone-responsive MA-10 mouse Leydig tumor cells were used to study the role of 14-3-3ε in steroidogenesis. Immunocytochemistry indicated that 14-3-3ε was present and partially colocalized with mitochondria in MA-10 mouse tumor Leydig cells (**Figure 1a**). Immunoblot analysis indicated that the cAMP analog 8-Bromo-cAMP (8-Br-cAMP), which triggers maximal steroidogenesis, did not alter 14-3-3ε levels in MA-10 cells after 120 minutes of treatment, which is a time point at which the increase in the rate of steroidogenesis is highest (**Figure 1b**), However, Blue-Native polyacrylamide gel electrophoresis followed by immunoblot of isolated mitochondrial complexes from hormone-treated MA-10 cells showed a fivefold induction in

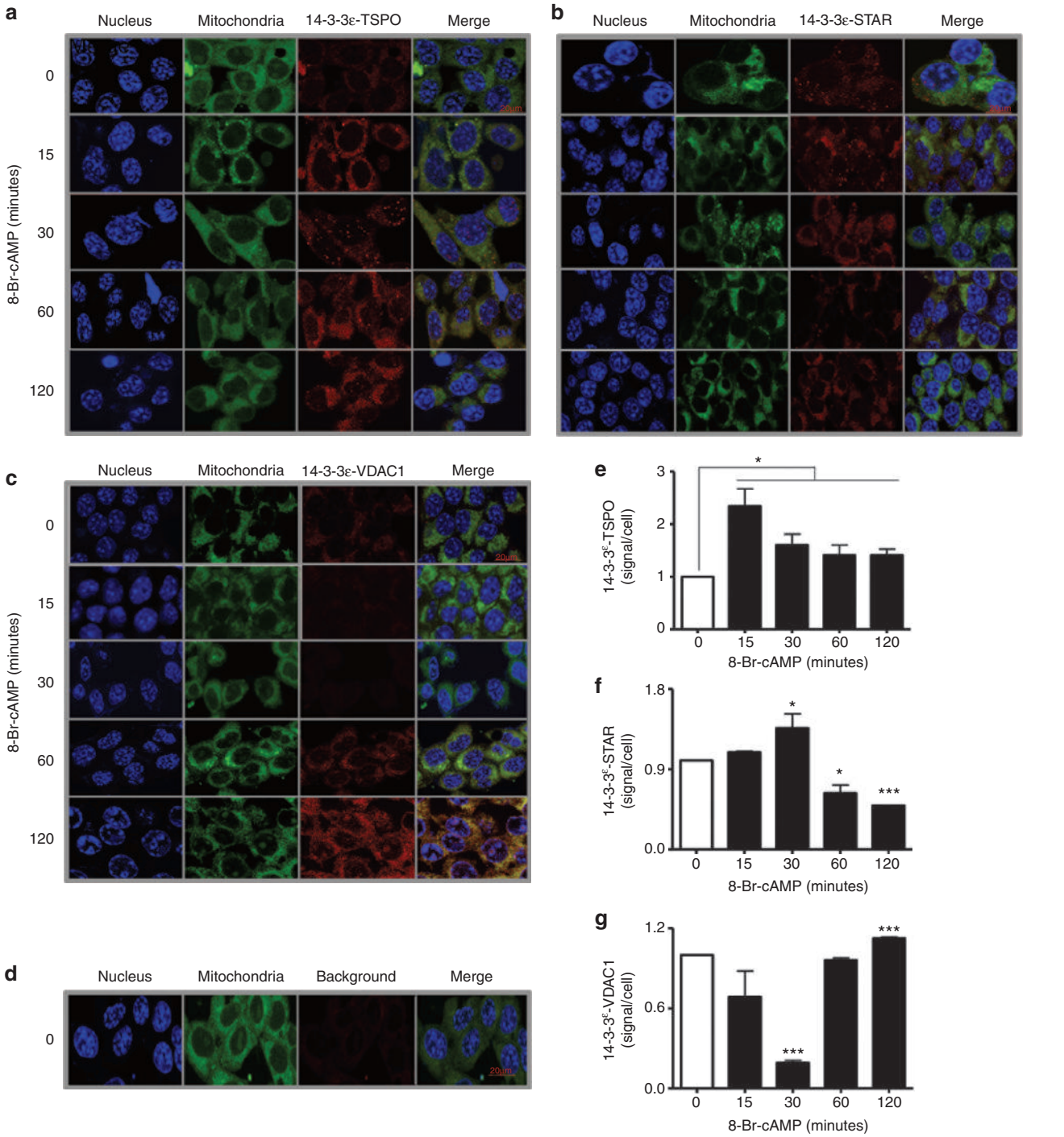

Figure 2 TSPO, STAR, and voltage-dependent anion channel (VDAC1) are targets of 14-3-3ε. (**a–d**) *In cell* immunoprecipitation (Duolink technology) indicates the dynamics of the interactions between 14-3-3ε with TSPO, STAR, and VDAC1. Images show the cell nucleus (blue), mitochondria (green), and endogenous protein–protein interactions (red) between 14-3-3ε-TSPO (**a**), 14-3-3ε-STAR (**b**), and 14-3-3ε-VDAC1 (**c**) the background signal (**d**) of the Duolink assay in MA-10 cells, and the merge of the three previous columns (**e–g**).

14-3-3ε levels compared to control; a finding confirmed by mass spectrometry of the isolated protein complexes.[19]

To understand the physiological role of 14-3-3ε in steroidogenesis, 14-3-3ε was knocked down with specific small interfering RNA (siRNA) (**Supplementary Figure S1**). Scrambled and hypoxanthine-guanine phosphoribosyl transferase (HPRT) siRNAs served as negative and positive controls, respectively. MA-10 cells were transfected with 5, 10, or 20 nmol/l siRNA to optimize knockdown (K/D). Ultimately, 10 nmol/l siRNA achieved 55–75% K/D of 14-3-3ε and was selected for transfection

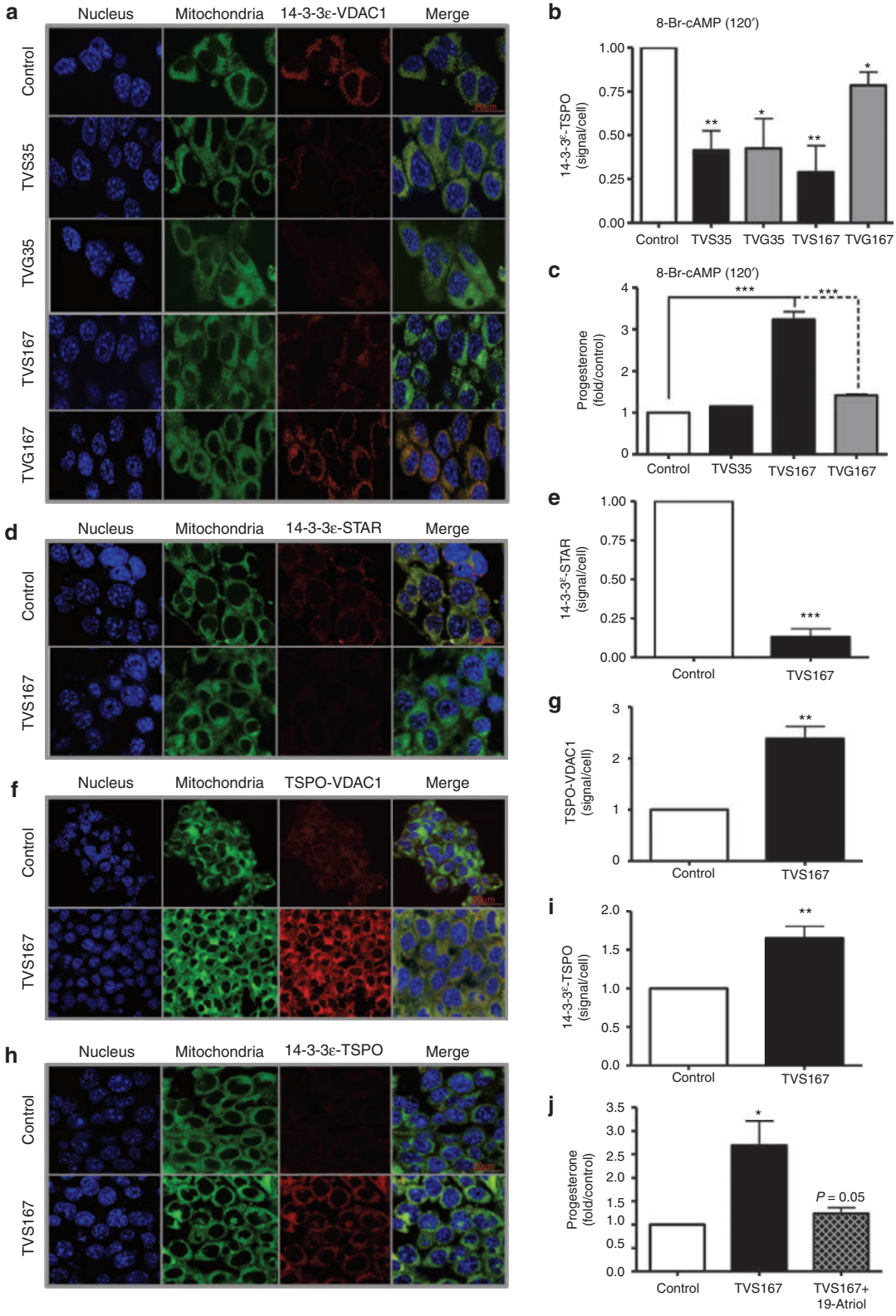

(Figure 1c). After transfecting 14-3-3ε siRNA, cells were treated with 8-Br-cAMP. Media were collected, and progesterone production was measured by radioimmunoassay. Treatment with 8-Br-cAMP for 120 minutes increased progesterone formation by threefold in cells with 14-3-3ε K/D compared to controls, suggesting that 14-3-3ε negatively regulated steroidogenesis (Figure 1d). These results suggest that, unlike 14-3-3γ, 14-3-3ε levels are not induced by hormone treatment and this protein may act as a negative regulator, blocking maximal steroid formation.

Identification of targets of 14-3-3ε negative regulation

In silico analysis of mouse TSPO, VDAC1, and STAR confirmed 14-3-3 binding motifs (mode I, RSXpSXP; mode II: RXXXpSXP) on TSPO adjacent to the CRAC domain,[19,25] on VDAC1 at its dimerization and lateral sites,[26] and on STAR at its cleavage and activation sites[12] (**Supplementary Figure S2a**). All motifs varied by one to two amino acids from the classic 14-3-3 motif, leading to high affinity but transient binding to 14-3-3 proteins.[27] To identify isoform-specific targets of 14-3-3ε, *in vitro* coimmunoprecipitation (co-IP) was performed using magnetic beads coupled with 14-3-3ε isoform-specific anti-sera[28] (**Supplementary Figure S2b**). MA-10 cells were treated with 8-Br-cAMP. Transient interactions between 14-3-3ε and target proteins[27] were strengthened by cross-linking with photo-activatable amino acids and ultraviolet (UV) light. Protein lysates precipitated with 14-3-3ε anti-sera were separated by sodium dodecyl sulfate–polyacrylamide gel electrophoresis, and interactions of 14-3-3ε with TSPO, STAR, and VDAC1 were assessed. Dimerization of 14-3-3ε was reduced by 8-Br-cAMP and reached a minimum after 120 minutes. Interactions between 14-3-3ε and TSPO were triggered by 8-Br-cAMP but were not time-dependent. In contrast, interactions between 14-3-3ε and STAR or VDAC1 peaked after 15–30 and 120 minutes, respectively (**Supplementary Figure S2b**). Co-IP did not appear to be sufficiently sensitive to capture 14-3-3ε targets, therefore, *in cell* IP[29] was performed. Interactions between 14-3-3ε and TSPO were triggered within 15 minutes of 8-Br-cAMP treatment and were maintained (Figure 2a,e). Interactions between 14-3-3ε and STAR increased at earlier time points but decreased after 120 minutes of 8-Br-cAMP treatment (Figure 2b,f). This pattern was opposite to that observed for 14-3-3ε and VDAC1, as these proteins had reduced interactions at earlier treatment times and significantly increased interactions at 120 minutes (Figure 2c,g). Interestingly, the negative regulatory function of 14-3-3ε in steroidogenesis was also observed at 120 minutes. Thus, VDAC1 appears to be a 14-3-3ε target and mediator of 14-3-3ε effects. The background signal is shown in Figure 2d.

Identification and manipulation of 14-3-3ε—VDAC1 interactions

To identify the 14-3-3ε-specific site of interaction with VDAC1, part of HIV transcription factor 1 (TAT) was fused with each of the *in silico*-predicted 14-3-3-binding motifs on VDAC1 to create TAT-VDAC1 Ser35 (TVS35) and TAT-VDAC1 Ser167 (TVS167) (**Supplementary Figure S3a**). The TAT sequence easily penetrates the cell membrane[30] and shuttles the conjugated peptide. Serine residues are important for 14-3-3 binding[23] and were mutated to create TAT-VDAC1 Gly35 (TVG35) and TAT-VDAC1 Gly167 (TVG167) control peptides. TVS167 was fluorescently labeled. Confocal microscopy indicated that 250 nmol/l TVS167 penetrated into all of the MA-10 cells within 90 minutes (**Supplementary Figure S3b**). MA-10 cells were then incubated in media with TV peptides. Maximal l4-3-3ε-VDAC1 interactions were induced by 120 minutes of 8-Br-cAMP treatment. Cells were fixed, and *in cell* IP studies were performed to measure interactions between 14-3-3ε and endogenous VDAC1 in the presence of each peptide. TVS35 and TVS167 competed with VDAC1 for binding 14-3-3ε, resulting in reduced interactions between endogenous 14-3-3ε and VDAC1 (Figure 3a,b). TVG35 also interacted with 14-3-3ε. However, TVG167-14-3-3ε interactions were much lower, allowing endogenous VDAC1 and 14-3-3ε to interact (Figure 3a,b).

Disruption of 14-3-3ε-VDAC1 interaction at S167, but not S35, induced steroid formation similar to that observed by 14-3-3ε K/D (Figure 3c). The interactions between 14-3-3ε-STAR and TSPO-VDAC1 were measured in the presence of TVS167 and 8-Br-cAMP. Disruption of VDAC1-14-3-3ε interaction inhibited binding of STAR to 14-3-3ε (Figure 3d,e), suggesting that VDAC1 and STAR interact with 14-3-3ε at the same site, explaining the opposite patterns of interactions between these proteins and 14-3-3ε (Figure 2b,c,f,g). Interestingly, TSPO-VDAC1 interactions were increased in the presence of TVS167. These data suggest that the 14-3-3ε scaffold intercalates between TSPO and VDAC1, blocking interactions that mediate cholesterol import across the OMM. Therefore, 14-3-3ε buffers cholesterol import to mitochondria (Figure 3f,g). TVS167 increased interactions between 14-3-3ε and TSPO by 1.6-fold (Figure 3h,i). Cholesterol binding to TSPO was blocked with 19-Atriol, a drug that targets the CRAC domain and decreases steroidogenesis.[31] The stimulatory effect of TVS167 was blocked by 19-Atriol, suggesting that interactions between 14-3-3ε and TSPO affected cholesterol binding to TSPO (Figure 3j). The binding of PK 11195, the most prominent TSPO drug ligand,[32] was altered showing increased affinity and reduced binding capacity (**Supplementary Figure S4**). Thus, 14-3-3ε appears to regulate the microenvironment of TSPO.

Figure 3 Blocking the interaction between 14-3-3ε and voltage-dependent anion channel (VDAC1) negates the regulatory role of 14-3-3ε in steroidogenesis. (**a**,**b**) The Duolink assay was performed to measure protein–protein interactions between 14-3-3ε and endogenous VDAC1 in untreated MA-10 cells (control) or cells treated with the TVS35, TVG35, TVS167, or TVS167 peptides, after 8-Br-cAMP (120 minutes) treatment, which induces maximum 14-3-3ε-VDAC1 interaction (red). Staining of nucleus (blue) and mitochondrial (green) are also shown. (**c**) Progesterone levels in control MA-10 cells or cells treated with TVS35, TVS167, or TVS167 were measured after 8-Br-cAMP (120 minutes) treatment. Levels of progesterone were normalized to protein content and further compared to the levels in control cells, as fold increase. (**d–g**,**i**,**j**) The impact of blocking interactions between 14-3-3ε-VDAC1 on other transduceosome protein–protein interactions was studied in the presence of TVS167. MA-10 cells were treated with TVS167 and 8-Br-cAMP (120 minutes). The interactions between 14-3-3ε-STAR (**d**,**e**), TSPO-VDAC1 (**f**,**g**), and 14-3-3ε-TSPO (**h**,**i**) were measured, as endogenous protein–protein interactions. Histograms show the sum of protein–protein interactions in Z-stacks as signal/cell ratio. (**j**) The physiological impact of the increase in 14-3-3ε-TSPO interactions on cholesterol binding to TSPO was studied. Progesterone levels in control (untreated), TVS167-treated, and combination 19-Atriol/TVS167-treated MA-10 cells were measured after 8-Br-cAMP stimulation (120 minutes).

Therefore, the interaction between 14-3-3ε and TSPO is critical for steroidogenesis.

TV peptides penetrate rat testes and induce T production *ex vivo* and *in vivo* in an LH-independent manner

Testes from adult Sprague-Dawley rats were collected and cultured *ex vivo* to assess the potential of the TAT-VDAC1 fusion (TV) peptides to penetrate the testes and induce Leydig cell androgen formation. Testes were maintained in media with 250 nmol/l TV peptides for 90 minutes followed by treatment with or without hCG for 120 minutes. TV peptides penetrated the rat testes, and TVS167 treatment induced T production (**Figure 4a**). Interestingly, testes treated with TVS167 produced significantly more T than hCG-treated controls. Rats were then injected in one testis with water, 150 ng TVG167, or 15, 150, 300, or 1,500 ng TVS167. The contralateral testis was used as a control. Blood and testes were collected 2 hours after injection, and T levels were measured in the intratesticular fluid and serum by radioimmunoassay. T levels increased in a dose-dependent manner in testes treated with TV peptides, whereas the contralateral testes of the same animals used as control, had reduced T levels. This trend began at 300 ng dose and reached significance with 1,500 ng TVS167, suggesting that LH negative feedback is triggered at these doses (**Supplementary Figure S5a**). Therefore LH levels were measured, showing that in the presence of 300–1,500 ng TVS167 increased T production led to the suppression of circulating LH levels (**Supplementary Figure S5b**). Thus, 150 ng TVS167, the highest dose that does not affect LH levels was further used. To induce and maintain T production over longer periods of time, a 150-ng bolus of T was injected into one testis of each rat. Alzet mini-osmotic pumps containing water (TV peptide diluent), TVG167, or TVS167 were surgically implanted in the abdomen and directed to the injected testis with a small catheter. The contralateral testis served as a control. Pumps released 75 ng TVS/G167 (250 nmol/l) over 24 hours. T levels in interstitial fluid and serum and also circulating LH levels were measured. Animals treated with TVS167 had significantly higher levels of T in interstitial fluid and serum, whereas LH levels were significantly reduced compared to controls (**Figure 4b–d**). *In vivo* VDAC1-14-3-3ε interactions were studied through *in cell* IP in the testes of control and rats implanted with water- or TVS167-releasing pumps. TVS167 treatment blocked 14-3-3ε-VDAC1 interactions (**Figure 4e**). No morphological differences were seen between rat testis from controls or from animals implanted with water or TVS167-releasing pumps (**Supplementary Figure S6**).

The *in vivo* induction of T by TVS167 is LH-independent

We examined if TVS167 triggers T production in animals with very low LH levels. The gonadotropin-releasing hormone antagonist Cetrorelix was intraperitoneally (i.p.) injected into 60–64-day-old rats at 0.4 mg/day for 4 days as previously described.[33] T levels

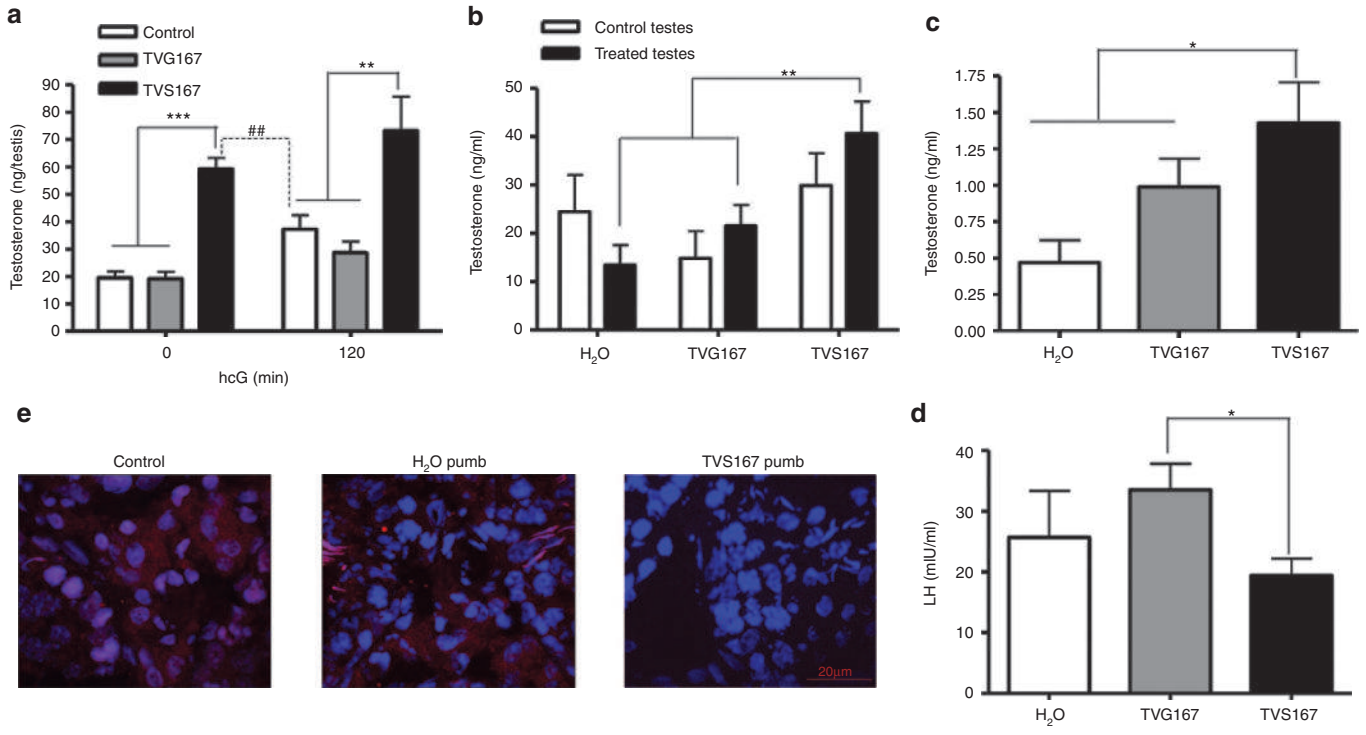

Figure 4 TVS167 administration modulates *in vivo* T production. (**a**) Testes dissected from adult Sprague-Dawley rats were cultured in media supplemented with or without TVG167 or TVS167 and/or hCG (120 minutes). T levels were measured. (**b–d**) Adult Sprague-Dawley rats were injected in one testis with water or 150 ng TVG167 or TVS167. A pump releasing H_2O, 75 ng/24 hours TVG167, or 75 ng/24 hours TVS167 was connected to the injected testis. Animals were dissected after 24 hours. Intratesticular T levels were measured in treated and control testes (**b**). Serum T levels (**c**) and serum LH levels (**d**) were also measured. (**e**) Duolink assay was performed on the testes sections. Immunofluorescence images show the merge of nucleus channel (blue) and protein–protein interaction channel (red) indicating that in the presence of TVS167 peptide, the interactions of 14-3-3ε and VDAC1 in rat testes are removed.

were completely suppressed in the testes and serum 4 days after injection (**Figure 5a,b**; no pump). Next, Cetrorelix was injected i.p. for 0–4 days while on day 3 animals were injected in one testis with 150 ng TVS167 and implanted with TVS167-releasing pump. Animals were sacrificed after 24 hours. T levels increased by 12-, 8-, or 20-fold, respectively, in testes connected to a TVS167 pump, testes not connected to a pump (due to diffusion) and in both testes together (**Figure 5a** +, –, total). TVS167 treatment increased circulating T by fivefold (**Figure 5b**).

To further assess the link between VDAC1 and TSPO function *in vivo*, the acute effect of TVS167 was compared to that of a the well characterized high affinity TSPO drug ligand, *N,N*-dihexyl-2-(4-fluorophenyl)indole-3-acetamide (FGIN-1–27),[34] in the absence of LH signaling. Sprague-Dawley rats of 68–72 days old were given an i.p. injected of either H_2O or 0.4 mg Cetrorelix for 0–4 days. On day 4, a bolus intratesticular injection of 8.5 µg FGIN-1–27 or its solvent (control) was given to one testis per animal. To assess the acute effect of this TSPO drug ligand on steroidogenesis, intratesticular and circulating T levels were measured after 2 hours. The results obtained showed a significant increase in intratesticular T levels in both control and Cetrorelix-treated rats (**Figure 5c**), whereas plasma T levels were increased only in the Cetrorelix-treated animals (**Figure 5d**). It should be noted that a 2 hours bolus intratesticular injection of TVS167 peptide to control Sprague-Dawley rats also resulted in an increase in circulating T levels (**Supplementary Figure S5a**).

Prediction of TVS167 binding to 14-3-3ε in different species

Sequence alignment showed high (>99%) homology between *Mus musculus*, *Homo sapiens*, and *Rattus norvegicus* 14-3-3ε and VDAC1 proteins. The VDAC1 14-3-3ε binding motif that contains S167 was conserved across species (**Supplementary Figure S7**). The three-dimensional (3-D) structures of human, mouse, and rat VDAC1 and 14-3-3ε were also highly conserved (**Figure 6a**). Protein–protein docking predicted the binding site of 14-3-3ε on VDAC1. Surface mapping of electrostatic potential in 14-3-3ε indicates that the VDAC1 binding site is involved in protein–protein interaction (**Figure 6b**). These data also indicate that S167 is in the mitochondrial membrane suggesting that the interactions of 14-3-3ε with this residue might decrease the conductance of VDAC1 which in turn could affect cholesterol

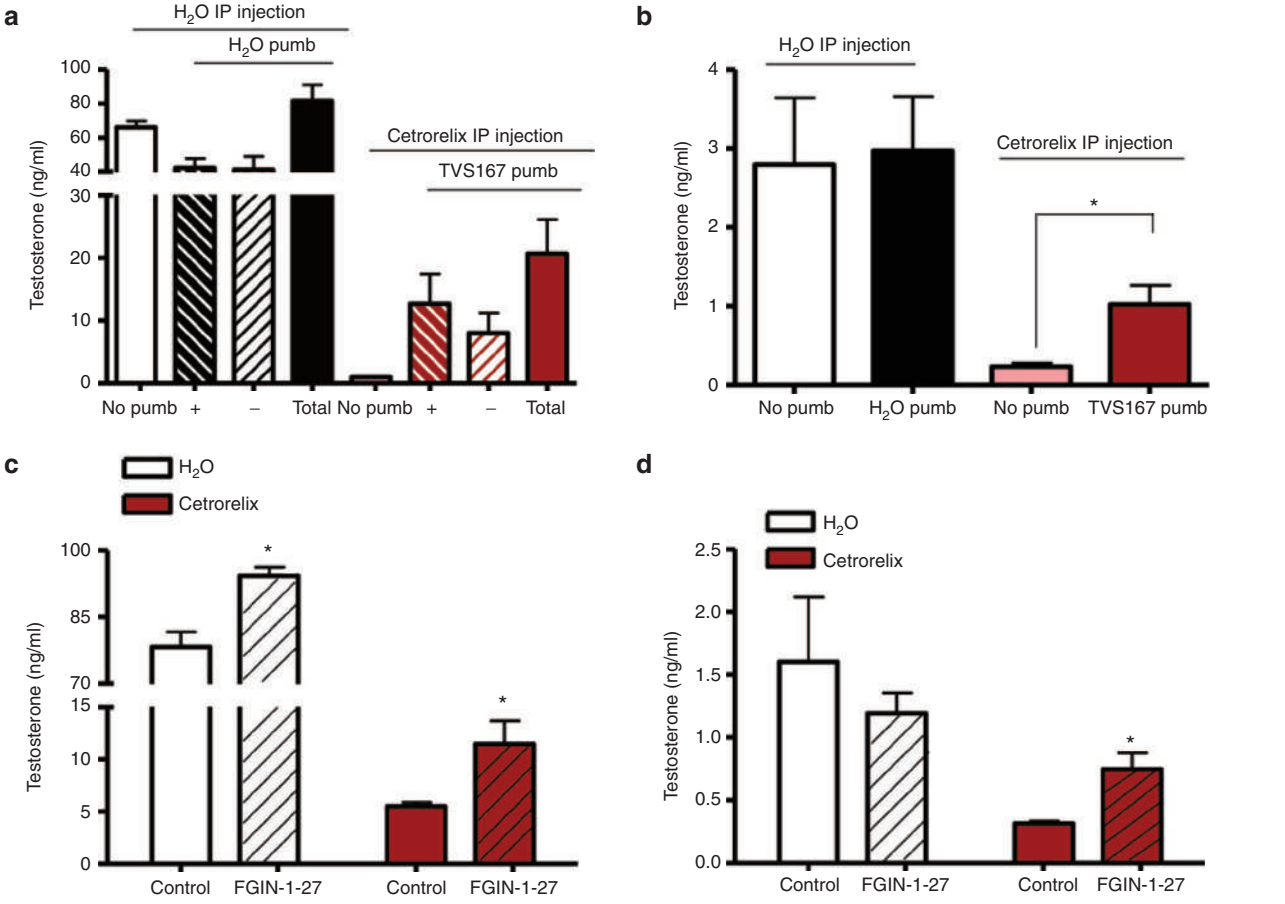

Figure 5 The effect of TVS167 *in vivo* is LH-independent. (**a**,**b**) Adult Sprague-Dawley rats were given i.p. injections of H_2O or Cetrorelix (0.4 mg/day). Animals were either dissected on day 4 (no pump) or treated with H_2O (if given H_2O i.p.) or TVS167 (if given Cetrorelix i.p.) through a bolus injection and pump installation to one testis and dissected 24 hours after pump installation. T levels in the intratesticular fluid (**a**) of testis connected to a pump (+), not connected to a pump (–), or both testes (no pump and Total) and in serum were measured (**b**). Adult Sprague-Dawley rats were injected i.p. with either H_2O or Cetrorelix for 0–4 days and on day 4, one testis per animal was given a bolus injection of 8.5 µg FGIN-1–27 to induce acute steroidogenesis in the absence or presence of LH signaling. T levels in intratesticular (**c**) and plasma (**d**) were measured 2 hours postinjection, showing a significant increase.

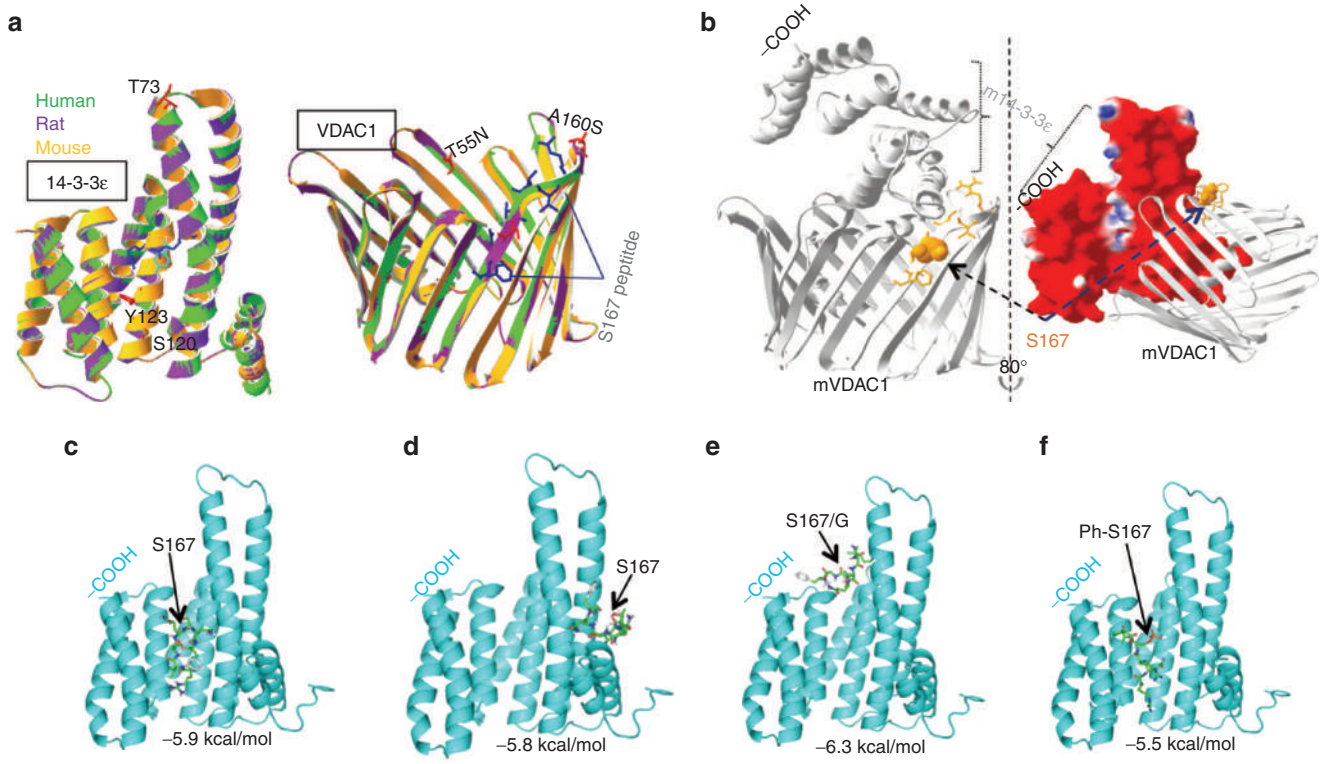

Figure 6 Modeling the human voltage-dependent anion channel (VDAC1) 14-3-3ε motif containing S167. (**a**) Putative models 14-3-3ε and VDAC1 were mapped in indicated species showing a high degree of homology. (**b**) Macromolecular docking among two proteins. The docking site of 14-3-3ε in the VDAC1 structure in *Mus musculus* was predicted. TVS167 was shown to dock onto open and non-ligand-bound 14-3-3ε at the site to which VDAC1 also bound to this protein, suggesting that TV167 can block this interaction. Due to a high percentage of homology between the 3-D structures of human 14-3-3ε and VDAC1, the same docking sites were predicted in these species. The ribbon representative of each protein and surface mapping of electrostatic potential of mouse 14-3-3ε are shown. The red, blue, and white on the molecular surface are corresponding to negative, positive, and neutral charged regions, respectively. (**c,d**) The molecular docking studies show TVS167 targets the 14-3-3ε binding groove as well as the right shoulder that interacts with VDAC1(6b). (**e**) Mutation of S167 to G167 removes the ability of the TV peptide to dock outside the binding groove. (**f**) The phosphorylated TVS167 docked within the binding groove.

transport. Molecular docking of 14-3-3ε with TVS167 shows the peptide binding within the binding groove with −5.9 kcal/mol affinity (**Figure 6c**) and to the right "shoulder" of the 14-3-3ε, the same site as VDAC1 binding site, with −5.8 kcal/mol affinity, (**Figure 6d**). Similar molecular docking studies indicated that if S167 is mutated to G, the TVG167 peptide falls out of the binding groove, indicating that the mutated peptide is not the favorable ligand of the protein (**Figure 6e**). As the most favorable binding site of 14-3-3 proteins to their targets occurs mostly at phosphorylated serine residues, docking studies were performed using the phosphorylated TVS167 peptide (Ph-S167) indicating that the top 9 conformations are all within the binding groove, with –5.5 kcal/mol affinity (**Figure 6f**). Therefore, the most favorable peptide ligand for 14-3-3ε is Ph-TVS167.

Specificity of TVS167 effects on testicular steroidogenesis

TAT peptides pass through all cell types,[30] and 14-3-3ε is ubiquitously expressed in mammalian tissues. However, expression levels and function of 14-3-3ε are tissue-specific. To gain insights into the effects of TVS167 in other steroid-synthesizing tissues, such as the adrenal gland, 14-3-3ε expression was studied in three mammalian species. Immunohistochemistry was performed on adult mouse testes and adrenals. Testicular interstitial cells were enriched with 14-3-3ε, whereas the levels and concentrations of 14-3-3ε were lower in the steroidogenic adrenal cortex (**Figure 7a**). In adult rats, levels of 14-3-3ε were significantly higher in testes than adrenals (**Figure 7b**). The effect of TVS167 on corticosterone production was examined in sera from rats implanted with TVS167-releasing pumps for 24 hours. Significantly higher intratesticular and circulating T levels were found compared to control rats implanted with water-releasing pumps (**Figure 4d,e**). Circulating corticosterone levels were not significantly changed by TVS167 (**Figure 7c**). Microarray data (http://biogps.org) indicated that 14-3-3ε mRNA levels were higher in human testes than human adrenals (**Figure 7d**). Similar to MA-10 cells, human adrenocortical NCL-H295R cells were treated with or without TVS167 followed by *in cell* IP to examine 14-3-3ε-VDAC1 interactions. Interactions between 14-3-3ε and VDAC1 were decreased by TVS167. However, this decrease was not significant, possibly because 14-3-3ε levels are lower in NCL-H295R cells (**Figure 7e**).

DISCUSSION

T contributes to quality-of-life and well-being.[1,2,35] Male development, virilization, sexual differentiation, and fertility rely on T production throughout life.[2,36] A progressive decline in T

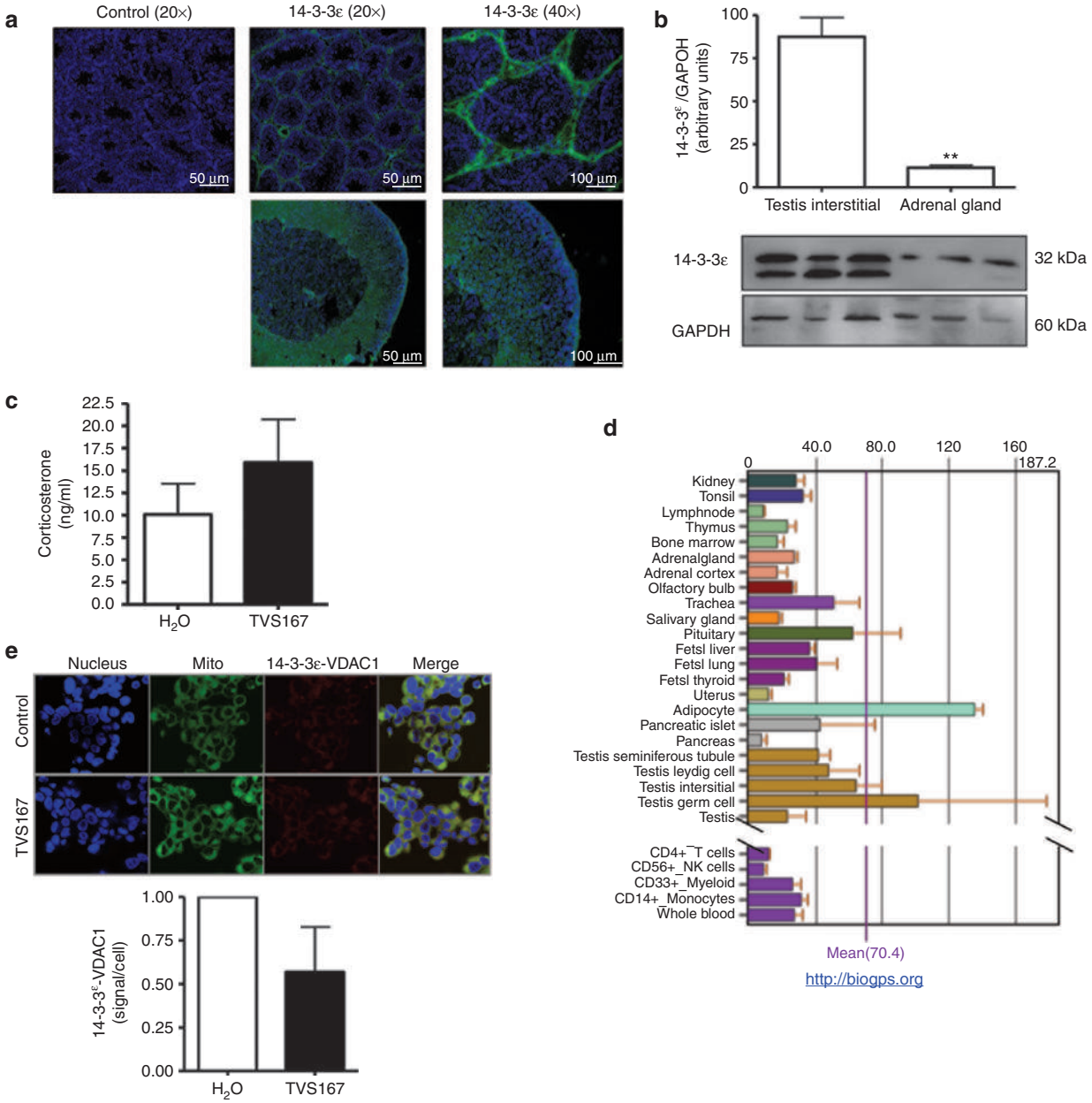

Figure 7 Comparison of 14-3-3ε protein profile in adrenal gland versus testis. (**a**) Immunofluorescence images illustrates the nucleus (blue) and 14-3-3ε expression (green) in sections of adult mice adrenal gland and testes indicating higher levels of protein expression in interstitial cells of testes compared to adrenal glands. (**b**) Immunoblot analysis shows that the expression levels of 14-3-3ε compared to GAPDH are significantly higher in protein lysate extracted from interstitial testes compared of adrenal glands of adult rats. (**c**) Adult rats were implanted with H_2O and TVS167 releasing pumps abdominally, this pump was directed to one testis and induces T levels in rat testes and plasma (Figure 4d–f). Corticosterone levels produced by the adrenal gland cortex were measured in these rats indicating insignificant changes compared to control. (**d**) Public microarray data comparing mRNA levels of 14-3-3ε in human tissues indicates higher mRNA in human interstitial cells compared to adrenal gland. (**e**) Duolink assay was performed to study the protein–protein interactions between 14-3-3ε and voltage-dependent anion channel (VDAC1) in NCL-H296R human adrenocortical cell line. Immunofluorescence images illustrate the nucleus (blue), mitochondria (green), and protein–protein interactions (red) indicating that the protein–protein interaction signal is not as high as in MA-10 cells and rat testes sections and that despite a decrease in the interactions of 14-3-3ε and VDAC1 in these cells in the presence of TVS167, this effect is not significant.

begins at age 40 (andropause) and continues in aging males.[1,35] This decline is due in part to an age-related reduction in steroidogenesis by testicular Leydig cells, *i.e.*, primary hypogonadism.[37] A low level of T has been linked with several chronic and life-threatening diseases and is also a major cause of male infertility.[2,5,6] TRT shows clinical benefit in patients with andropause in order to ameliorate muscle mass and strength, bone density, libido and quality of erection. However, TRT is not recommended for patients with non-treated or at high risk of prostate cancer, breast cancer, sleep apnea, infertility, cardiovascular problems, and hematocrit over 50%.[1,6,8,35,38] Therefore, alternative therapies with fewer side effects are needed. We examined

endogenous mechanisms to develop an approach to induce steroid formation, ideally in an LH-independent manner.

The transduceosome mediates the rate-limiting step of steroidogenesis, which is cholesterol import from the cytosol to the mitochondria.[11,16] Defects in aging Leydig cells involve this rate-limiting step.[39] We speculated that a scaffold protein at the OMM allows spatial and temporal regulation of protein–protein interactions, leading to cholesterol import and steroid formation. We previously reported that 14-3-3ε is present in the mitochondria of steroidogenic cells.[19] Induction of steroidogenesis triggered movement of 14-3-3ε from the cytosol to the OMM. K/D studies indicated that 14-3-3ε is a negative regulator of steroidogenesis and a potential target for inducing T biosynthesis. 14-3-3ε is primarily in the cytosol associated with STAR at the beginning of steroidogenesis. VDAC1 then competes with STAR to bind to 14-3-3ε. This promotes relocalization of 14-3-3ε to mitochondria and intercalation between TSPO and VDAC1, resulting in reduced cholesterol import into mitochondria. We believe that competition between STAR and VDAC1 for 14-3-3ε binding balances the interactions between TSPO and 14-3-3ε. Disruption of this balance affects the TSPO microenvironment, which disrupts the binding of cholesterol to this protein. Negative regulation by 14-3-3ε occurs in response to interactions with VDAC1. S167 on VDAC1 was the critical amino acid for these interactions. Analyses of *in cell* protein–protein interactions indicated that TVS167 competed with endogenous VDAC1 to reduce interactions with 14-3-3ε, leading to increased steroidogenesis. Consequently, serum levels of T were elevated. However, this increase was not as pronounced as that observed in testes. Thus, this approach did not jeopardize the ability of testes to retain T and allowed a controlled amount of T to be released into circulation.

Gonadotropin-releasing hormone antagonists induce chemical castration by removing LH signaling and blocking T production. Cetrorelix blocked LH release and T production in adult rats. Testicular infusion of TVS167 to the testes of Cetrorelix-treated rats increased T by 20-fold despite a lack of LH. Thus, protein–protein interactions are critical for the production of T by Leydig cells in the absence of LH. These results suggest that TVS167 is a potential therapy for treating primary hypogonadism and for maintaining physiological T levels during situations, such as aging, without requiring exogenous administration of T.

The data presented point to TSPO as the downstream target of the 14-3-3ε-VDAC interactions mediating cholesterol delivery into mitochondria for steroidogenesis. Indeed, TVS167 affected the 14-3-3ε-TSPO interactions, increased the TSPO drug ligand affinity while reducing its binding capacity, and the stimulatory effect of TVS167 on steroid formation was blocked by 19-Atriol, a drug blocking cholesterol binding to TSPO. Moreover, FGIN-1–27, a high affinity TSPO drug ligand induced acute T formation *in vivo* both in control and Cetrorelix-treated rats, although to a lesser extent than TVS167, in agreement with recent findings in aged Brown-Norway rat Leydig cells, a model of male hypogonadism.[40]

Although the signal transduction mechanisms mediating the effect of LH on Leydig cell steroidogenesis are well known, this work suggests that alternative mechanisms via intracellular peptide mediators may be involved in the production of T. The presence of such natural intracellular peptides able to regulate protein–protein interactions and cell signal transduction was recently demonstrated.[41,42]

Homo sapiens, *Mus musculus*, and *Rattus norvegicus* 14-3-3ε and VDAC1 proteins showed high degrees of homology. In addition, the VDAC1 14-3-3ε binding motif that contains S167 had a 100% across-species homology. Thus, it is highly probable that the bioactive peptides that we developed will also induce T formation in humans. In fact, surface mapping of 14-3-3ε indicated that TVS167 binds to the open structure of 14-3-3ε and blocks docking of 14-3-3ε to VDAC1 in all species.

The adrenal is second only to the gonads as a major site of steroid synthesis. Although these tissues share common signaling mechanisms for regulating steroid formation, there are some differences. For example, different lipoproteins supply cholesterol for steroidogenesis, and the adrenal has a rapid stress response to hormones.[43] Tissue-specific roles of 14-3-3ε are well-established, 14-3-3ε levels were much lower in the adrenals than in the testes. In addition, interactions between 14-3-3ε and VDAC1 were lower in human adrenocortical cells compared to testes. Moreover, TVS167 significantly increased circulating T levels in rats but failed to induce corticosteroid levels. These results demonstrate the specificity of TVS167 for maintaining testicular function and T formation without affecting the adrenal steroidogenesis.

Taken together, the results presented herein not only unveiled a novel mechanism regulating androgen biosynthesis but also identified a novel therapeutic target which upon activation allows for the recovery of the ability of the testis to form androgens. Thus, the identified lead peptide TVS167 offers a new potential means for treating primary hypogonadism and for maintaining physiological T levels when needed, without requiring exogenous administration of T. Considering that in addition to androgens, the testis makes a number of other physiologically important steroids, it is obvious that activating the endogenous mechanism of steroid production in testis may offer additional benefits to the administration of a testosterone analog.

Materials and methods

Cell culture, treatments, and steroid measurement. MA-10 mouse Leydig tumor cells (kindly provided by Dr M Ascoli, University of Iowa, Ames, IA) were maintained in Dulbecco's modified Eagle's medium/Ham's nutrient mixture F12 (Gibco, Burlington, ON) supplemented with 5% fetal bovine serum, 2.5% hoarse serum, and 1% penicillin and streptomycin at 37 °C, and 3.7% CO_2. Cells were incubated in serum-free cell culture media supplemented with 1 mmol/l 8-Bromo-cAMP (Enzo Biosciences, Farmingdale, NY) or 1.36 µmol/l (50 ng/ml) hCG (kindly provided by Dr AF Parlow, the National Hormone & Peptide Program, Harbor-UCLA Medical Center, Los Angeles, CA) for 15, 30, 60, and 120 minutes or as indicated. Human NCL-H295R cells (kindly provided by Dr William E Rainey, Department of Physiology, Medical College of Georgia, Augusta, GA) were maintained in Dulbecco's modified Eagle's medium/F12 media supplemented with 2.5% Ultroser G (Pall Biospera, Mississauga, ON), 1% penicillin/streptomycin (Invitrogen, Carlsbad, CA), and 1% ITS+ Premix (BD Biosciences, Franklin Lakes, NJ) in a humidified chamber at 37 °C and 5% CO_2.

Experiments involving the TV peptides included 1×10^3 MA-10 or NCL-H295R cells, which were initially cultured for 24 hours. Serum-free media were supplemented with 250 nmol/l TV fusion peptides, and cells were incubated for 90 minutes after optimization. For the experiments

with 19-Atriol, 1×10^3 MA-10 cells were cultured for 24 hours. Serum-free media were supplemented with 10 µmol/l 19-Atriol and, and cells were treated for 120 minutes.[39]

In the siRNA transfection studies, 4×10^5 MA-10 cells were plated in gelatin-coated 100-mm cell culture dishes and incubated for 24 hours. Cells were transfected with 5, 10, or 20 nmol/l of a mixture of three predesigned siRNA (IDT, San Jose, CA) sequences (**Supplementary Figure S1**) using Lipofectamine RNAiMAX (Invitrogen) and Opti-MEM transfection medium. Dulbecco's modified Eagle's medium/F12 culture media without antibiotics was added to reach 5 ml for the 72-hour incubation period. HPRT siRNA and scrambled siRNA were transfected at 10 nmol/l each and served as positive and negative control, respectively (IDT). The optimum concentration of 14-3-3ε siRNA, which was used for further studies, was 10 nmol/l siRNA (**Supplementary Figure S1**), which achieved 55–75% K/D (**Supplementary Figure S1**).

Progesterone or testosterone levels were measured with specific radioimmunoassays in triplicate using commercial anti-sera from rabbit and sheep, respectively (MP Biomedicals, Santa Ana, CA). Protein levels in MA-10 cell lysates were determined with the Bradford dye assay (Bio-Rad, Hercules, CA). LH and corticosterone levels were measured with rat-specific ELISA kits (CUSABIO, Wuhan, China).

Animals studies. Animals were handled according to protocols approved by the McGill University Animal Care and Use Committees. Sixty- to 64-day-old male Sprague-Dawley rats were purchased from Charles River, Senneville, QC. Rats were provided standard diets and tap water *ad libitum* and were maintained in controlled conditions (24 °C, 12-hour light, 12-hour dark schedule). Animals were euthanized, and the testes were either immediately used for organ culture or intratesticular fluid collection, or testes and adrenal glands were snap-frozen for sectioning. Bolus injections with water or indicated doses of TV peptides were performed after administering isofluorane anesthesia. Rats were injected with either water or the indicated dose of TV fusion peptide. When FGIN-1–27 (Sigma-Aldrich, St Louis, MO) was used, 8.5 µg in 50 µl (390 µmol/l) of the compound in 1% dimethyl sulfoxide solution containing Tween-20 was injected into one of the testes of 68–72-day-old Sprague-Dawley rats. Animals were incubated in standard conditions for 2 hours. Surgeries were performed on 60- to 64-day-old rats bolus injection of water or TV peptides. Alzet mini-osmotic pumps releasing 75 ng of filled with water or a TV peptide or water over a course of 24 hours was surgically implanted in the abdomen. The pumps were connected to a polyethylene catheter tubing (Alzet) and directed to the injected testis. The pump released 75 ng TV peptide to the testis over a course of 24 hours at the rate of 1 µl/hour. Gonadotropin-releasing hormone antagonist, Cetrorelix (Sigma-Aldrich) was injected into 59-day-old rats i.p. at 0.4 mg/animal/day for 0–4 days.[33] Animal dissection was performed after CO_2 anesthesia. Cardiac puncture was used for blood collection, and further centrifugation yielded serum separation. Testes were dissected and either decapsulated for intratesticular fluid collection or snap-frozen for sectioning.

Ex vivo *organ culture.* Sixty- to 64-day-old Sprague-Dawley rats were dissected. Testes were collected, weighed, and decapsulated. A gentle mechanical disruption was performed, keeping the tubular structures intact. Testes were cultured in Dulbecco's modified Eagle's medium/F12 media with or without 250 nmol/l TV peptides and incubated for 90 minutes with or without 1.36 µmol/l hCG at 3.7% CO_2 and 34 °C.

Immunocytochemistry and confocal microscopy. MA-10 cells (2×10^4) were plated in 96-well glass-bottom dishes (Fluorodish) in triplicate until 60% confluent. Time–course treatments with 1 mmol/l cAMP followed by Cells were fixed in 4 °C methanol for 3–5 minutes, permeabilized with 10% Triton X-100 for 3 minutes, and blocked with 10% goat serum for 1 hour. 14-3-3ε antibody (1:50) and VDAC1 antibody (1:140, Abcam, Cambridge, UK) were added overnight at 4 °C. The wells were washed the next day with 1× phosphate-buffered saline and incubated in secondary anti-mouse IgG F(ab')$_2$ Fragment (Alexa Fluor 488 Conjugate, Green) and anti-rabbit IgG F (ab')$_2$ Fragment (Alexa Fluor 555 Conjugate, Red) (Cell Signaling Technology, Danver, MA) for 1 hour. Cells were washed, DAPI was added for nuclear staining, and cells were maintained in ultra-pure water. Confocal microscopy was performed with an Olympus Fluoview FV1000 Laser Confocal Microscope at 100× magnification.

Immunohistochemistry. Testes and adrenal glands from adult mice were purchased from Cytochem, Montreal, QC. Fluorescent staining was performed on testes and adrenal sections after fixing the tissues as previously explained.[19] Briefly, sections were permeabalized with 1% Triton X-100, blocked with 10% goat serum in 1% bovine serum albumin for 1 hour, and incubated with 14-3-3ε antibody (1:50) overnight at 4 °C in a humidity chamber. The following day, cells were washed in 1× phosphate-buffered saline and incubated with and secondary anti-mouse IgG F(ab')$_2$ Fragment (Alexa Fluor 488 Conjugate, Green; Invitrogen) for 1 hour. Hoechst (Enzo Biosciences) was used for nuclear staining. Sections were maintained in one drop of mounting media (Invitrogen), and Images were captured with an Olympus inverted microscope with 20× and 40× lenses. Hematoxylin staining was performed on testes sections from 60- to 64-day-old Sprague-Dawley rats 24 hours postpump implantation surgery. Tissues were snap-frozen and sectioned to be 4–6-µm thick (Cytochem).

Immunoblot analysis. Immunoblot analysis was performed on protein lysates of MA-10 cells and testicular interstitial cells and adrenal glands from 60-day-old Sprague-Dawley rats. Briefly, for MA-10 cell lysate extraction, 6×10^5 cells were cultured in six-well gelatin-coated plates in triplicate for 24 hours and treated with cAMP for a time course. Cells were washed with 1× phosphate-buffered saline and harvested. For testicular interstitial cell lysates, testes were decapsulated, mechanically disrupted in RPMI 1640 media (Sigma-Aldrich), and incubated in media containing 0.05% collagenase/dispase (Roche Diagnostics, Basel, Switzerland), 0.005% soybean trypsin inhibitor, and 0.001% deoxyribonuclease I (Sigma-Aldrich) for 20 minutes at 34 °C. The supernatant was collected, filtered, and centrifuged at 900 rpm for 10 minutes at 25 °C. The Leydig-cell-enriched pellet was snap-frozen until further use. Adrenal glands were snap-frozen for later use. MA-10 cell pellets, interstitial cells, and adrenal glands were mechanically homogenized in RIPA lysis buffer (Cell Signaling Technology), and protein levels were measured by the Bradford protein assay (Bio-Rad). MA-10 protein lysate (10 µg) and interstitial or adrenal protein lysates (15 µg) were solubilized and immunoblot was performed as previously described.[19]

In silico *prediction of the presence of the 14-3-3 binding motif.* The presence of the following types of 14-3-3 binding motifs were assessed manually in *Mus musculus* VDAC1, TSPO, and STAR: mode I, RSXpSXP; mode II: RXXXpSXP, in which R is Arginine, S is serine, X is any amino acid, P is proline, and T is threonine; mode III: pS/pTX$_{1\text{-}2}$- CO_2 H, in which X is not proline.[27]

Cross-linking studies. MA-10 cells (1×10^6) were plated in gelatin-coated 100-mm Petri cell culture dishes overnight. Media were replaced with Dulbecco's modified Eagle's limiting media supplemented with 10% fetal bovine serum and 105 mg/l photo-leucine and 30 mg/l photo-methionine (Thermo Scientific, Waltham, MA). Cells were incubated for 22 hours followed by cAMP time–course treatment. Crosslinking was performed immediately after each time point with a 3UV lamp (UVP) for 16 minutes at 365 nm at a distance of 1 cm from the surface of the Petri dishes.

Coimmunoprecipitation. Coimmunoprecipitation was performed with Dynabeads Co-Immunoprecipitation Kit (Invitrogen). The 14-3-3ε-specific antibody[28] was coupled with the dynabeads, yielding 10 mg/ml of antibody-coupled beads according to the manufacturer's instructions. Crosslinked MA-10 protein lysates were harvested in extraction buffer

A (1× immunoprecipitation buffer, 1 mol/l NaCl, and protease inhibitor without ethylenediaminetetraacetic acid), and 0.15 or 0.5 mg protein was precipitated with 14-3-3ε antibody-coupled beads rotating at 4 °C for 1 hour to study 14-3-3ε dimerization or target binding, respectively. The precipitated samples were loaded onto 4–20% Tris-glycine gels. MA-10 cell lysate (10 µg) was used as a control. Immunoblotting was performed as previously described with the following antibodies: anti-14-3-3 pan (1:1,000, Santa Cruz Biotechnology, Santa Cruz, CA), anti-TSPO (1:1,000 dilution),[44] anti-STAR (1:5,000 dilution, kindly provided by Dr B Hales, University of Southern Illinois, IL),[45] and anti-VDAC1 (2 µg/ml, Abcam).

In cell IP and confocal microscopy. Duolink technology was used[29] for *in cell* IP. In this assay, primary antibodies raised in different species were incubated with cells or tissue sections of interest. Species-specific secondary antibodies were conjugated to short oligonucleotide tails, which form a circular oligonucleotide strand upon addition of a ligase. A polymerase was added to amplify this nucleotide strand followed by addition of a fluorescent tag, which hybridizes with this strand. Fluorescent signals were captured by confocal microscopy and measured with O-link software. MA-10 cells were cultured at 1×10^3 per well, in a 96-well glass-bottom dish (Fluorodish, Sarasota, FL) in triplicate and incubated overnight. The next day, cells were treated with cAMP and immediately fixed after each time point in 3.7% formaldehyde for 15 minutes. Sections of adult rat testes were obtained and fixed in 3.7% formaldehyde for 20 minutes. Fixed MA-10 cells and sections of rat testes were washed and permeabilized with 1% Triton X-100 for one minute. Duolink II Red Starter Kit (OLink Biosciences, Uppsala, Sweden) was used according to the manufacturer's instructions. MA-10 cells were incubated with a combination of mouse anti-14-3-3ε (1:150) and either rabbit anti-STAR (1:150), rabbit anti-TSPO (1:150), or rabbit anti-VDAC1 (1:140) or with a different combination of rabbit anti-TSPO and mouse anti-VDAC1 (1:140) overnight at 4 °C. A combination of mouse anti-14-3-3ε and rabbit anti-VDAC1 was used for rat tissue sections. Mitochondria and nuclei were stained with Mito-ID and Hoechst, respectively (Enzo Biosciences) for 30 minutes at 37 °C. MA-10 cells were maintained in Ultra-pure water, and tissue sections were maintained in one drop of mounting media. Protein–protein interactions were detected with Olympus Fluoview FV1000 Laser Confocal Microscope at ×100 magnification. *Z*-stacks were captured from the bottom to the top of MA-10 cell nuclei. The sum of signals from all *Z*-stacks were measured with O-link software and divided by the number of cells in the corresponding image to obtain the signal/cell ratio for a minimum of 60 cells. One image of each of the rat sections was captured from the middle of the nucleus, which is the area of maximum focus with the 100× lens.

Radioligand binding assays. Binding of [^{3}H]-PK 11195 to 5 mg MA-10 cell homogenate was performed as described previously.[46] Specific [^{3}H]-PK 11195 binding was analyzed with the iterative nonlinear curve-fitting program in GraphPad Prism 5.

TV peptide design and labeling. TV Peptides were designed with an 11-mer of the HIV-1 virus trans-activator of transcription protein (TAT)[30] followed by a glycine residue and amino acids 28–40 (containing 14-3-3 motif KTKSEN) or amino acids 160–172 (containing 14-3-3 motif RVTQSNF) of mVDAC1. Serine residues in 14-3-3 motifs are important for 14-3-3 binding. Thus, peptides were named according to the serine residue in the peptide. TAT-VDAC1 fusion peptide S35 was named TVS35, and TAT-VDAC1 fusion peptide S167 was named TVS167. S35 and S167 were mutated to glycine residues as controls, and TVG35 and TVG167 were synthesized. TVS167 was labeled with 6-fluorescein (FAM) 488. Peptide synthesis and labeling were outperformed at the Sheldon Biotechnology Center, McGill University, Montreal, QC. Peptide sequences are shown in **Supplementary Figure S3a**.

Protein sequence alignment, homology modeling, and molecular docking. The amino acid sequences for the 14-3-3ε and VDAC1 proteins in *Mus musculus, Homo sapiens*, and *Rattus norvegicus* were aligned using ClustalW.[47] The selected VDAC1 14-3-3 binding motif containing S167 was conserved between these three species. Coordinates of human and mouse VDAC1 and human 14-3-3ε were from the Brookhaven Protein Database (PDB: 2JK4 and 3EMN for VDAC1; 2BR9 for 14-3-3ε).[48] The coordinates of the putative three-dimensional structure of mouse 14-3-3ε in the absence of ligand were predicted via an automated comparative protein modeling server (Swiss-Model, Basel, Switzerland) (http://www.expasy.ch) at the University of Geneva. The optimized mode used the coordinates of the human 14-3-3γ protein (PDB: 4E2E) as a template. The putative 3-D structures of the rat VDAC1 and 14-3-3ε proteins were predicted in a similar fashion using mouse VDAC1 (PDB: 3EMN) and human 14-3-3ε (PDB: 2BR9) as templates, respectively.[49] The 3-D coordinates of the TVS167 peptide (phosphorylated and nonphosphorylated) were prepared with the PyMOL Molecular Graphics System V. 1.3 (Schrödinger, Portland, OR). The 3D coordinates of the Ph-TVS167 were extracted from the crystal structure of human 14-3-3ε in complex with phospho-peptide ligand (PDB: 2BR9), and then virtually mutated. Docking of the peptide with the 14-3-3ε protein was performed with AutoDock-vina.[50] Protein–protein docking between mouse VDAC1 and 14-3-3ε was performed with HEX V 6.3. All docking results and protein structures are presented either in the PyMOL Molecular Graphics System and/or in Swiss-PDB viewer 4.1.

Statistical analysis. Experimental results were examined for significance by two-tailed *t*-tests (**Figures 1b**,**c**, **2f**,g,3b,c,e,g,i,j, 4b,c,f, 5a,b and 7b,c) or one-way analysis of variance (**Figures 1d**, **2e** and 3a,e,f) with GraphPad Prism 5 software. Cells from three independent passages ($n = 3$) were included for each experiment that involved MA-10 and NCL-H295R cells, and each passage was examined in triplicate in each experiment. In the *ex vivo* testes cultures, three and four animals were included for the control and TVS167 or TVG167 treatment respectively ($n = 3$ or $n = 4$). For bolus dose–response testicular injections, three animals were used for each dose ($n = 3$). Five animals ($n = 5$) were included for each pump installation of different groups involving water, TVS167, or TVS167-releasing pumps. Three animals ($n = 3$) were included per group for i.p. injections of water or Cetrorelix. Six animals ($n = 6$) were included per group for water or Cetrorelix injections followed by water or TVS167 pump installation.

SUPPLEMENTARY MATERIAL

Figure S1. Sequences of 14-3-3ε specific siRNA.
Figure S2. 14-3-3ε interactions with other 14-3-3 isoforms, TSPO, STAR, and VDAC1 identified *in silico* and *in vitro* by cross-linking immunoprecipitation.
Figure S3. Sequence of TV fusion peptides.
Figure S4. 14-3-3ε regulates the affinity of TSPO for its drug ligand PK11195.
Figure S5. TVS167 induces T levels in a dose response manner.
Figure S6. Administration of the TVS167 peptides does not induce toxic histological modifications to the testis.
Figure S7. Alignment of amino acid sequences of 14-3-3ε and VDAC1 showing high degree of conservation for both proteins and that the 14-3-3 binding motif is conserved in the three mammalian species as indicated.

ACKNOWLEDGMENTS

We thank Mario Ascoli (University of Iowa) for the MA-10 cell line, AF Parlow (National Hormone & Peptide Program, Harbor-UCLA Medical Center) for supplying hCG, Buck Hales (Southern Illinois University) for the STAR antibody, and William E Rainey (Medical College of Georgia) for supplying NCL-H295R cells. We also thank Charles Essagian and Annie Boisvert for expert assistance with the animal studies. This work was supported by grants from the Canadian Institutes of Health Research (MOP102647 and 125983) and a Canada Research Chair in Biochemical Pharmacology to V.P. Y.A. was supported in part by

predoctoral fellowships from the Research Institute of MUHC and the McGill Center for the Study of Reproduction. The Research Institute of MUHC was supported by a Center grant from Le Fonds de la recherche du Québec-Santé. Y.A. designed the project, conducted the experiments, analyzed the data, and wrote the manuscript. D.B.M.A. designed and performed the animal surgeries. J.F. performed the modeling studies. M.C. conceived the study and provided overall supervision. V.P. conceived the study, designed the project, analyzed data, supervised the overall project, and wrote the manuscript. D.B.M.A. and M.C. declare that they have no competing financial interests. Y.A., J.F., and V.P. are named coinventors on a patent filed with U.S.P.T.O.

REFERENCES

1. Huhtaniemi, I and Forti, G (2011). Male late-onset hypogonadism: pathogenesis, diagnosis and treatment. *Nat Rev Urol* **8**: 335–344.
2. Carruthers, M (2009). Time for international action on treating testosterone deficiency syndrome. *Aging Male* **12**: 21–28.
3. Lang, PO, Samaras, D and Samaras, N (2012). Testosterone replacement therapy in reversing "andropause": what is the proof-of-principle? *Rejuvenation Res* **15**: 453–465.
4. Guay, AT, Spark, RF, Bansal, S, Cunningham, GR, Goodman, NF, Nankin, HR *et al.*; American Association of Clinical Endocrinologists Male Sexual Dysfunction Task Force. (2003). American Association of Clinical Endocrinologists medical guidelines for clinical practice for the evaluation and treatment of male sexual dysfunction: a couple's problem–2003 update. *Endocr Pract* **9**: 77–95.
5. Bhasin, S, Cunningham, GR, Hayes, FJ, Matsumoto, AM, Snyder, PJ, Swerdloff, RS *et al.*; Task Force, Endocrine Society. (2010). Testosterone therapy in men with androgen deficiency syndromes: an Endocrine Society clinical practice guideline. *J Clin Endocrinol Metab* **95**: 2536–2559.
6. Wang, C, Nieschlag, E, Swerdloff, R, Behre, HM, Hellstrom, WJ, Gooren, LJ *et al.* (2009). Investigation, treatment and monitoring of late-onset hypogonadism in males. *Int J Androl* **32**: 1–10.
7. Twiddy, AL, Leon, CG and Wasan, KM (2011). Cholesterol as a potential target for castration-resistant prostate cancer. *Pharm Res* **28**: 423–437.
8. Vigen, R, O'Donnell, CI, Barón, AE, Grunwald, GK, Maddox, TM, Bradley, SM *et al.* (2013). Association of testosterone therapy with mortality, myocardial infarction, and stroke in men with low testosterone levels. *JAMA* **310**: 1829–1836.
9. Ferrini, RL and Barrett-Connor, E (1998). Sex hormones and age: a cross-sectional study of testosterone and estradiol and their bioavailable fractions in community-dwelling men. *Am J Epidemiol* **147**: 750–754.
10. de Ronde W (2009). Hyperandrogenism after transfer of topical testosterone gel: case report and review of published and unpublished studies. *Hum. Reprod.* **24**, 425–428.
11. Papadopoulos, V, Liu, J and Culty, M (2007). Is there a mitochondrial signaling complex facilitating cholesterol import? *Mol Cell Endocrinol* **265–266**: 59–64.
12. Miller, WL (2007). StAR search–what we know about how the steroidogenic acute regulatory protein mediates mitochondrial cholesterol import. *Mol Endocrinol* **21**: 589–601.
13. Papadopoulos, V, Baraldi, M, Guilarte, TR, Knudsen, TB, Lacapère, JJ, Lindemann, P *et al.* (2006). Translocator protein (18kDa): new nomenclature for the peripheral-type benzodiazepine receptor based on its structure and molecular function. *Trends Pharmacol Sci* **27**: 402–409.
14. Jamin, N, Neumann, JM, Ostuni, MA, Vu, TK, Yao, ZX, Murail, S *et al.* (2005). Characterization of the cholesterol recognition amino acid consensus sequence of the peripheral-type benzodiazepine receptor. *Mol Endocrinol* **19**: 588–594.
15. Li, H and Papadopoulos, V (1998). Peripheral-type benzodiazepine receptor function in cholesterol transport. Identification of a putative cholesterol recognition/interaction amino acid sequence and consensus pattern. *Endocrinology* **139**: 4991–4997.
16. Liu, J, Rone, MB and Papadopoulos, V (2006). Protein-protein interactions mediate mitochondrial cholesterol transport and steroid biosynthesis. *J Biol Chem* **281**: 38879–38893.
17. Bose, M, Whittal, RM, Miller, WL and Bose, HS (2008). Steroidogenic activity of StAR requires contact with mitochondrial VDAC1 and phosphate carrier protein. *J Biol Chem* **283**: 8837–8845.
18. Hauet, T, Yao, ZX, Bose, HS, Wall, CT, Han, Z, Li, W *et al.* (2005). Peripheral-type benzodiazepine receptor-mediated action of steroidogenic acute regulatory protein on cholesterol entry into leydig cell mitochondria. *Mol Endocrinol* **19**: 540–554.
19. Aghazadeh, Y, Rone, MB, Blonder, J, Ye, X, Veenstra, TD, Hales, DB *et al.* (2012). Hormone-induced 14-3-3γ adaptor protein regulates steroidogenic acute regulatory protein activity and steroid biosynthesis in MA-10 Leydig cells. *J Biol Chem* **287**: 15380–15394.
20. Umahara, T, Uchihara, T, Nakamura, A and Iwamoto, T (2011). Differential expression of 14-3-3 protein isoforms in developing rat hippocampus, cortex, rostral migratory stream, olfactory bulb, and white matter. *Brain Res* **1410**: 1–11.
21. Gupta, P, Ho, PC, Huq, MD, Khan, AA, Tsai, NP and Wei, LN (2008). PKCepsilon stimulated arginine methylation of RIP140 for its nuclear-cytoplasmic export in adipocyte differentiation. *PLoS One* **3**: e2658.
22. Pozuelo, RM, Geraghty, KM, Wong, BH, Wood, NT, Campbell, DG, Morrice, N *et al.* (2004). 14-3-3-affinity purification of over 200 human phosphoproteins reveals new links to regulation of cellular metabolism, proliferation and trafficking. *Biochem J* **379**, 395–408.
23. Aitken, A (2006). 14-3-3 proteins: a historic overview. *Semin Cancer Biol* **16**: 162–172.
24. Alam, R, Hachiya, N, Sakaguchi, M, Kawabata, S, Iwanaga, S, Kitajima, M *et al.* (1994). cDNA cloning and characterization of mitochondrial import stimulation factor (MSF) purified from rat liver cytosol. *J Biochem* **116**: 416–425.
25. Li, H, Yao, Z, Degenhardt, B, Teper, G and Papadopoulos, V (2001). Cholesterol binding at the cholesterol recognition/ interaction amino acid consensus (CRAC) of the peripheral-type benzodiazepine receptor and inhibition of steroidogenesis by an HIV TAT-CRAC peptide. *Proc Natl Acad Sci USA* **98**: 1267–1272.
26. Geula, S, Naveed, H, Liang, J and Shoshan-Barmatz, V (2012). Structure-based analysis of VDAC1 protein: defining oligomer contact sites. *J Biol Chem* **287**: 2179–2190.
27. Yaffe, MB, Rittinger, K, Volinia, S, Caron, PR, Aitken, A, Leffers, H *et al.* (1997). The structural basis for 14-3-3:phosphopeptide binding specificity. *Cell* **91**: 961–971.
28. Gegenbauer, K, Elia, G, Blanco-Fernandez, A and Smolenski, A (2012). Regulator of G-protein signaling 18 integrates activating and inhibitory signaling in platelets. *Blood* **119**: 3799–3807.
29. Fredriksson, S, Gullberg, M, Jarvius, J, Olsson, C, Pietras, K, Gústafsdóttir, SM *et al.* (2002). Protein detection using proximity-dependent DNA ligation assays. *Nat Biotechnol* **20**: 473–477.
30. Nagahara, H, Vocero-Akbani, AM, Snyder, EL, Ho, A, Latham, DG, Lissy, NA *et al.* (1998). Transduction of full-length TAT fusion proteins into mammalian cells: TAT-p27Kip1 induces cell migration. *Nat Med* **4**: 1449–1452.
31. Midzak, A, Akula, N, Lecanu, L and Papadopoulos, V (2011). Novel androstenetriol interacts with the mitochondrial translocator protein and controls steroidogenesis. *J Biol Chem* **286**: 9875–9887.
32. Le, FG, Perrier, ML, Vaucher, N, Imbault, F, Flamier, A, Benavides, J *et al.* (1983). Peripheral benzodiazepine binding sites: effect of PK 11195, 1-(2-chlorophenyl)-N-methyl-N-(1-methylpropyl)-3-isoquinolinecarboxamide. I. In vitro studies. *Life Sci* **32**: 1839–1847.
33. Horvath, JE, Toller, GL, Schally, AV, Bajo, AM and Groot, K (2004). Effect of long-term treatment with low doses of the LHRH antagonist Cetrorelix on pituitary receptors for LHRH and gonadal axis in male and female rats. *Proc Natl Acad Sci USA* **101**: 4996–5001.
34. Romeo, E, Auta, J, Kozikowski, AP, Ma, D, Papadopoulos, V, Puia, G *et al.* (1992). 2-Aryl-3-indoleacetamides (FGIN-1): a new class of potent and specific ligands for the mitochondrial DBI receptor (MDR). *J Pharmacol Exp Ther* **262**: 971–978.
35. Perheentupa, A and Huhtaniemi, I (2009). Aging of the human ovary and testis. *Mol Cell Endocrinol* **299**: 2–13.
36. Feldman, HA, Longcope, C, Derby, CA, Johannes, CB, Araujo, AB, Coviello, AD *et al.* (2002). Age trends in the level of serum testosterone and other hormones in middle-aged men: longitudinal results from the Massachusetts male aging study. *J Clin Endocrinol Metab* **87**: 589–598.
37. Saad, F (2009). The role of testosterone in type 2 diabetes and metabolic syndrome in men. *Arq Bras Endocrinol Metabol* **53**: 901–907.
38. Valero, RJ, Marquez, LJ, Campos, HP, Puigvert, MA and Prieto, CR (2013). Current recommendations about the diagnosis and treatment of testosterone deficit syndrome: clinical guidelines. *Arch Esp Urol* **66**: 737–744.
39. Papadopoulos, V, Carreau, S and Drosdowsky, MA (1985). Effect of phorbol ester and phospholipase C on LH-stimulated steroidogenesis in purified rat Leydig cells. *FEBS Lett* **188**: 312–316.
40. Chung, JY, Chen, H, Midzak, A, Burnett, AL, Papadopoulos, V and Zirkin, BR (2013). Drug ligand-induced activation of translocator protein (TSPO) stimulates steroid production by aged brown Norway rat Leydig cells. *Endocrinology* **154**: 2156–2165.
41. Ferro, ES, Hyslop, S and Camargo, AC (2004). Intracellular peptides as putative natural regulators of protein interactions. *J Neurochem* **91**: 769–777.
42. Russo, LC, Asega, AF, Castro, LM, Negraes, PD, Cruz, L, Gozzo, FC *et al.* (2012). Natural intracellular peptides can modulate the interactions of mouse brain proteins and thimet oligopeptidase with 14-3-3ε and calmodulin. *Proteomics* **12**: 2641–2655.
43. Gwynne, JT and Strauss, JF 3rd (1982). The role of lipoproteins in steroidogenesis and cholesterol metabolism in steroidogenic glands. *Endocr Rev* **3**: 299–329.
44. Li, H, Degenhardt, B, Tobin, D, Yao, ZX, Tasken, K and Papadopoulos, V (2001). Identification, localization, and function in steroidogenesis of PAP7: a peripheral-type benzodiazepine receptor- and PKA (RIalpha)-associated protein. *Mol Endocrinol* **15**: 2211–2228.
45. Hales, KH, Diemer, T, Ginde, S, Shankar, BK, Roberts, M, Bosmann, HB *et al.* (2000). Diametric effects of bacterial endotoxin lipopolysaccharide on adrenal and Leydig cell steroidogenic acute regulatory protein. *Endocrinology* **141**: 4000–4012.
46. Papadopoulos, V, Mukhin, AG, Costa, E and Krueger, KE (1990). The peripheral-type benzodiazepine receptor is functionally linked to Leydig cell steroidogenesis. *J Biol Chem* **265**: 3772–3779.
47. Thompson, JD, Gibson, TJ, Plewniak, F, Jeanmougin, F and Higgins, DG (1997). The CLUSTAL_X windows interface: flexible strategies for multiple sequence alignment aided by quality analysis tools. *Nucleic Acids Res* **25**: 4876–4882.
48. Trott, O and Olson, AJ (2010). AutoDock Vina: improving the speed and accuracy of docking with a new scoring function, efficient optimization, and multithreading. *J Comput Chem* **31**: 455–461.
49. Ritchie, DW and Venkatraman, V (2010). Ultra-fast FFT protein docking on graphics processors. *Bioinformatics* **26**: 2398–2405.
50. Kramer, B, Rarey, M and Lengauer, T (1997). CASP2 experiences with docking flexible ligands using FlexX. *Proteins* (suppl. 1): 221–225.